ORIGINAL ARTICLE

# Tumor Atelectasis Gives Rise to a Solid Appearance in Pulmonary Adenocarcinomas on High-Resolution Computed Tomography

Francesca Ambrosi, MD,[a] Birgit Lissenberg-Witte, PhD,[b] Emile Comans, MD, PhD,[c] Ralf Sprengers, MD, PhD,[c] Chris Dickhoff, MD, PhD,[d] Idris Bahce, MD, PhD,[e] Teodora Radonic, MD, PhD,[f] Erik Thunnissen, MD, PhD[f,*]

[a]*Experimental, Diagnostic, and Specialty Medicine Department, University of Bologna Medical Center, Bologna, Italy*
[b]*Department of Epidemiology and Biostatistics, Amsterdam UMC, location VUmc, Amsterdam, the Netherlands*
[c]*Department of Radiology and Nuclear Medicine, Amsterdam UMC, location VUmc, Amsterdam, the Netherlands*
[d]*Department of Surgery and Cardiothoracic Surgery, Amsterdam UMC, location VUmc, Amsterdam, the Netherlands*
[e]*Department of Pulmonology, Amsterdam UMC, location VUmc, Amsterdam, the Netherlands*
[f]*Department of Pathology, Amsterdam UMC, location VUmc, Amsterdam, the Netherlands*

Received 11 February 2020; accepted 11 February 2020
Available online - 27 February 2020

## ABSTRACT

**Introduction:** Ground-glass opacities in a high-resolution computed tomography (HR-CT) scan correlate, if malignant, with adenocarcinoma in situ. The solid appearance in the HR-CT is often considered indicative of an invasive component. This study aims to compare the radiologic features revealed in the HR-CT and the histologic features of primary adenocarcinomas in resection specimens to find the presence of tumor atelectasis in ground-glass nodules (GGNs) and part-solid and solid nodules.

**Methods:** HR-CT imaging was evaluated, and lung nodules were classified as GGNs, part-solid nodules, and solid nodules, whereas adenocarcinomas were classified according to WHO classification. Lepidic growth pattern with collapse was considered if there was reduction of air in the histologic section with maintained pulmonary architecture (without signs of pleural or vascular invasion).

**Results:** Radiologic and histologic features were compared in 47 lesions of 41 patients. The number of GGN, part-solid, and solid nodules were two, eight, and 37, respectively. Lepidic growth pattern with collapse was observed in both GGN, seven of the eight part-solid (88%) and 24 of the 37 solid (65%) lesions. Remarkably, more than 50% of the adenocarcinomas with a solid appearance in HR-CT imaging had a preexisting pulmonary architecture with adenocarcinoma with a predominant lepidic growth pattern. In these cases, the solid component can be explained by tumor-related collapse in vivo (tumor atelectasis on radiologic examination).

**Conclusions:** Tumor atelectasis is a frequent finding in pulmonary adenocarcinomas and may beside a ground glass opacity also result in a solid appearance in HR-CT imaging. A solid appearance on HR-CT cannot be attributed to invasion alone, as has been the assumption until now.



*Keywords:* Adenocarcinoma; Atelectasis; Collapse; HR-CT; Pathology

***Corresponding author.**

***Disclosure: The authors declare no conflict of interest.***

**Address for correspondence: Erik Thunnissen, MD, PhD, Department of Pathology, Amsterdam UMC, location VUmc, De Boelelaan 1117, 1081 HV Amsterdam, the Netherlands. E-mail: e.thunnissen@amsterdamumc.nl**

**Cite this article as: Ambrosi F, et al. Tumor Atelectasis Gives Rise to a Solid Appearance in Pulmonary Adenocarcinomas on High-Resolution Computed Tomography. JTO Clin Res Rep 1:100018**



**ISSN: 2666-3643**

**https://doi.org/10.1016/j.jtocrr.2020.100018**

## Introduction

Lung cancer causes around 1.6 million tumor-related deaths per year.[1] The recommended imaging techniques to characterize a nodular lesion in the lung are high-resolution computed tomography (HR-CT) and fluorodeoxyglucose (FDG) positron emission tomography (PET).[2] Nodular lesions in the imaging findings are generally classified as (1) ground-glass opacities (GGOs), characterized by an increase in lung attenuation with preservation of bronchial and vascular structures; (2) ground-glass nodules (GGNs) with a partial solid component; and (3) solid nodules (SNs).[3] A subsolid nodule implies cases of GGO or GGN. The visual capacity of experienced radiologists to differentiate between GGO and GGN larger than 10 mm in persistent and transient nodules is moderate.[4]

The resolution of HR-CT is around 2 mm and allows an anatomical comparison to histologic characteristics at the level of secondary lobules[5] with interlobular septa as boundaries and in the center of the lobule the bronchovascular bundle.[6]

In 2011, the International Association for the Study of Lung Cancer, the American Thoracic Society, and the European Respiratory Society introduced the concept of adenocarcinoma in situ (AIS) and minimally invasive adenocarcinoma (MIA) in the classification of adenocarcinoma of the lung. AIS is a small and localized adenocarcinoma ($\leq$3 cm) characterized by exclusively lepidic growth, which respects the preexisting alveoli, with no evidence of vascular and pleural invasion or papillary or micropapillary structures. MIA is defined as a single nodule ($\leq$3 cm) characterized by a predominant lepidic pattern and less than or equal to 5 mm invasion.[7]

The solid component in lung nodules revealed in HR-CT imaging can predict invasive malignancy.[8-10] Radiologic and histologic comparison revealed that the solid component (adenocarcinoma $>$ 2.0 cm with $>$ 0.25 consolidation) was associated with the invasive component of adenocarcinoma.[10-12] Furthermore, according to Kudo et al.,[13] the radiologic features of different lung nodules were compared with the International Association for the Study of Lung Cancer, the American Thoracic Society, and the European Respiratory Society classifications of small lung adenocarcinomas and identified consolidation size as factors for predicting histologic invasion. Nevertheless, other results highlighted the importance of the proportion of GGO as a predictor of less invasive lung cancer.[14,15] The study of Lim et al.[16] on 46 subsolid nodules did not report any recurrence or metastasis at 3 years or 5 years of follow-up. This result may imply that these lesions are of low malignant potential or even preinvasive.

An additional explanation for the different results observed may be that the solid component in GGN and SN occurs because of the collapse of the adenocarcinoma with a predominant lepidic growth pattern. Currently, tumor collapse is not taken into account in the histologic classification of adenocarcinomas.[7,17]

The aim of this study was to perform a radiologic-pathologic association and explore the presence of a collapse in lepidic adenocarcinoma in GGN and SN revealed in HR-CT imaging. To this end, resection specimens of a 2-year period were evaluated.

## Materials and Methods

### Study Population

In a retrospective study, radiologic and pathologic revisions were performed on patients with resected primary adenocarcinoma of the lung diagnosed between November 2016 and November 2018 at the Department of Pathology, Amsterdam University Medical Centers, location VUmc. Patients who underwent neoadjuvant treatment were excluded. The study included resections from 44 patients. The HR-CT images of three referred patients could not be retrieved from the digital archive and were excluded from all analyses. This study was approved by the Amsterdam UMC, location VUmc's Institutional Review Board (2017.023).

### Methods

**Radiologic Examination.** A chest radiologist (RS) and nuclear medicine physician (EC), blinded to the pathologic results, evaluated the CT scans and FDG PET-CT imaging. The HR-CT scans were performed on a 256-slice CT scanner (Brilliance iCT, Philips Healthcare, Best, the Netherlands) with a collimation of 128 mm $\times$ 0.625 mm. The tube current was set at a reference of 180 mA/slice at 120 kV, modulating current per slice according to body habitus. PET-CT scans (PET acquisition at 60 min post-FDG injection) were performed on a 64-slice scanner (Ingenuity TF, Philips Healthcare, Best, the Netherlands) with a collimation of 64 mm $\times$ 0.625 mm and a similar tube current setting. The CT findings were analyzed in the lung window setting. A total of 41 chest HR-CT and 39 PET-CT scans in the 41 patients were evaluated for CT morphologic analysis of GGO, GGN, and SN. CT and PET-CT findings that were analyzed for each lesion included (1) location, (2) total size of the lesion(s), (3) size of the solid component (in pulmonary window, CT thickness slides range [0.9–2.5]), (4) central/peripheral in the lobe, (5) multiplicity (solitary/multiple), (6) margins (smooth, spiculate, or lobulated), (7) shape (round, polygonal, or irregular), (8) CT contrast enhancement, (9) pleural retraction, (10)

**Table 1.** Parameters for Histologic Evaluation

| | Choices for Each Parameter | | | | |
|---|---|---|---|---|---|
| Histologic classification | AIS<br>MIA<br>IA | | | | |
| Maximum tumor size (mm) | | | | | |
| Maximum size of invasive component (mm) | | | | | |
| Histologic pattern of IA | Lepidic % | Papillary % | Micropapillary % | Cribriform % | Solid % |
| Necrosis | Yes | | | No | |
| Collapse | Yes (mild, moderate, and severe) | | | No, absent | |
| Macrophages in alveolar spaces[a] | Yes | | | No | |
| Bronchiolar invasion | Yes | | | No | |
| Pleural invasion | PL0 | | PL1 | PL2 | PL3 |
| Lymph-node(s) | N0 | N1 | N2 | N3 | |
| Maximum size of lymph-node metastasis (mm) | | | | | |

[a]In areas with lepidic growth pattern.
AIS, adenocarcinoma in situ; MIA, minimally invasive adenocarcinoma; IA, invasive adenocarcinoma; PL, pleural invasion categories (0–3).

presence of concomitant air bronchogram, (11) cavities or bullae in the lesion, (12) visual FDG uptake, (13) standardized uptake value (SUV) maximum, (14) SUV mean, and (15) lymph-node size.

**Histologic Examination.** Two pathologists (ET and FA), blinded to radiologic and clinical information, reviewed all the slides (hematoxylin and eosin) of each patient. In case of discordance, a consensus was obtained. The morphologic parameters considered for each nodule are shown in Table 1 (the gross size of each tumor was retrieved from the gross pathologic report). The histologic diagnosis was made according to the 2015 WHO classification,[7] and the cribriform pattern was interpreted as solid.[18] The invasion of tumor in pleura, vessels, airway, or lung parenchyma was evaluated in hematoxylin and eosin stains/with elastic stain (Elastic Van Gieson).[19] According to the VUmc standard protocol for lung examination, all the specimens were freshly received and injected with and fixed in high volume 10% neutral-buffered formalin.[20]

Adenocarcinomas were staged according to the American Joint Committee on Cancer cancer staging guidelines.[21] Microscopically, the presence of collapse was noted in adenocarcinomas with a lepidic growth pattern, which revealed a reduction of air in the preexisting alveolar spaces lined by tumor cells (Fig. 1). In addition, the tumor did not invade vessels, septa, or bronchi(oli). Alveolar septa were sometimes thickened by lymphocytic infiltration, but there was no desmoplastic stroma reaction observed.

**Statistical Analysis.** Associations between the pathologic and radiologic categorical features were tested with a chi-square test (or a Fisher's exact test in case of two dichotomous features); associations between a categorical and a continuous variable were tested with the Mann-Whitney *U* test or the Kruskal-Wallis test. Associations between continuous variables were tested with Spearman's rank correlation. Data were described by frequency for categoric variables and by median and range for continuous variables. All analyses were performed by BLW[22] in SPSS version 22 (IBM Corp., Armonk, NY). *P* values less than 0.05 were considered statistically significant.

## Results

The HR-CT scans of 41 patients were reviewed. The clinical data are shown in Supplementary Table 1. Two nodules each were identified in four patients and three nodules in one patient. In two patients, the second nodule was not surgically removed. For two referred patients, the PET-CT images could not be retrieved. The associations between the HR-CT images and histologic features were assessed for 47 nodules as were the associations between PET-CT images and histologic features for 43 nodules. The associations between histologic types and radiologic parameters are shown in Table 2.

### *Pathology*

Histologic revision was performed in all 41 patients, and 47 nodules were identified. Histopathologic characteristics and associations with the histologic type are shown in Supplementary Table 2. Tumor collapse was found in 33 of 47 nodules (70.2%) and identified in all stages.

### *Radiologic-Pathologic Correlation*

The associations among radiologic findings (radiologic classification of the nodule, margins, semiquantitative FDG uptake values [visual evaluation], and the largest measurement of the solid component of the nodule) and histologic features (histologic classification of adenocarcinoma, collapse, the histologic pattern of growth, and the largest measurement of the invasive component) are shown in Table 3 and Figures 2 and 3.

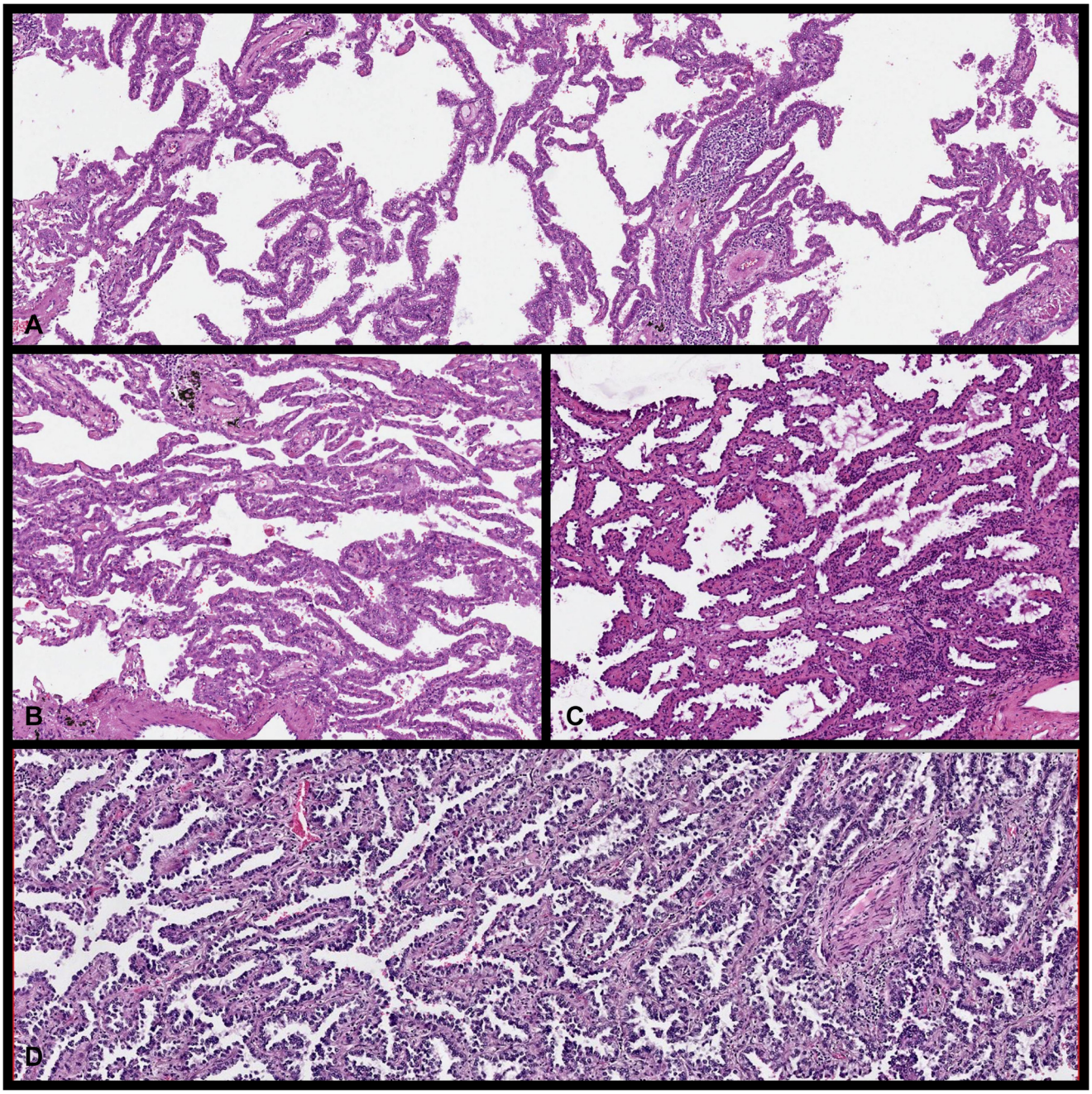


**Figure 1.** Histologic examples of peripheral lung tissue with tumor growth along alveolar walls and variation in collapse. (*A*) Histology (hematoxylin and eosin, ×50 magnification) of case without radiologic solid appearance (radiology not shown); (*B*, *D*) hematoxylin and eosin stain (×50, ×50, ×100 magnification, respectively) of cases with radiologic solid appearance (radiology not shown); and (*C*) macrophages in the alveolar spaces. Note the reduction in air spaces (*A*-*D*) with more prominent collapse.

Collapse was identified in 90.0% (nine of 10) of the tumors with a ground-glass component (GGO and GGN) and in 69.1% (29 of 42) of the SN ($p = 0.29$).

The measurement of the solid component in HR-CT imaging was associated with the histologic size of the invasive component ($p = 0.003$). The largest radiologic nodular size was associated with tumor necrosis ($p = 0.011$), pleural invasion ($p = 0.039$), bronchiolar invasion ($p = 0.020$), and the maximum size of the invasive component ($p = 0.006$). Macrophages in alveolar spaces, in the predominantly lepidic growth pattern component of the adenocarcinoma, were identified in 15 of the 47 nodules, and this histologic feature was associated with the radiologic classification of nodules (GGO, GGN, and SN, $p = 0.001$).

**Table 2.** Association Between Histologic Classification and Radiologic Parameters

| | Histologic Classification of Adenocarcinoma | | | |
|---|---|---|---|---|
| Radiologic Features | AIS | MIA | IA | *p* Value |
| Location | | | | |
| RUL | 0 | 2 | 13 | 0.19 |
| RML | 1 | 0 | 1 | |
| RLL | 0 | 1 | 5 | |
| RUL + RML + RLL | 0 | 0 | 1 | |
| RUL + RML | 0 | 0 | 1 | |
| LUL | 1 | 0 | 11 | |
| LLL | 0 | 0 | 10 | |
| Classification | | | | |
| GGO | 1 | 0 | 1 | 0.020 |
| GGN | 0 | 0 | 8 | |
| Solid | 1 | 3 | 33 | |
| Margins of the nodule(s) | | | | |
| Smooth | 1 | 0 | 1 | 0.018 |
| Spiculated | 0 | 1 | 30 | |
| Lobulated | 1 | 2 | 9 | |
| No margins | 0 | 0 | 2 | |
| Shape of the nodule(s) | | | | |
| Round | 0 | 0 | 2 | 0.18 |
| Polygonal | 2 | 0 | 8 | |
| Irregular | 0 | 3 | 30 | |
| No margins | 0 | 0 | 2 | |
| Largest size of the nodule(s) (mm) | | | | |
| Median (range) | 36 (28-44) | 16 (8-22) | 28 (4-250) | 0.28 |
| Largest size solid component (mm) | | | | |
| Median (range) | 44 (44-44) | 16 (8-22) | 23 (4-250) | 0.36 |
| Pleural retraction | | | | |
| Yes | 1 | 2 | 23 | 0.51 |
| No | 1 | 0 | 14 | |
| Air bronchogram | | | | |
| Yes | 1 | 0 | 6 | 0.37 |
| No | 1 | 2 | 31 | |
| Cavities, bulla | | | | |
| Yes | 1 | 0 | 6 | 0.37 |
| No | 1 | 2 | 31 | |
| Lymph-node involvement | | | | |
| Yes | 0 | 0 | 11 | 0.43 |
| No | 2 | 2 | 25 | |
| Visual FDG uptake[a] | | | | |
| No uptake | 1 | 0 | 0 | <0.001 |
| Faint | 0 | 0 | 8 | |
| Moderate | 1 | 1 | 3 | |
| Intense | 0 | 1 | 27 | |

[a]FDG uptake was addressed as a semiquantitative evaluation.
RUL, right upper lobe; RML, right middle lobe; RLL, right lower lobe; LUL, left upper lobe; LLL, left lower lobe; GGO, ground-glass opacity; GGN, ground-glass nodule; SN, solid nodule; AIS, adenocarcinoma in situ; MIA, minimally invasive adenocarcinoma; IA, invasive adenocarcinoma; FDG, fluorodeoxyglucose.

Radiologic lymph-node involvement was associated with pathologic node status ($p = 0.002$), lymph vascular invasion ($p = 0.030$), and the maximum size of the invasive component ($p = 0.037$); pathologic lymph-node metastasis was found only in patients with SN (40.5%).

The visual analysis of the FDG uptake (no uptake, faint, moderate, and intense uptake) was associated with AIS, MIA, and IA ($p < 0.001$). The $SUV_{max}$ and $SUV_{mean}$ values were associated with the presence of macrophages in alveolar spaces ($p = 0.027$ and $p = 0.025$, respectively).

## Discussion

This radiologic-pathologic comparison reveals that tumor atelectasis in HR-CT is the solid part in partially or

**Table 3.** Distribution of Pathologic Features for HR-CT and PET-CT

| | Radiologic Classification of Nodules | | | | Margins on HR-CT | | | | | Visual FDG Uptake[a] | | | | | Size of the Solid Component on HR-CT (mm) | |
|---|---|---|---|---|---|---|---|---|---|---|---|---|---|---|---|---|
| Histologic parameters | GGO | GGN | SN | *p* Value | SM | SP | LB | No M | *p* Value | NU | F | MOD | INT | *p* Value | Median (range) | p Value |
| Histologic classification | | | | | | | | | | | | | | | | |
| AIS | 1 | 0 | 1 | 0.003 | 1 | 0 | 1 | 0 | 0.024 | 1 | 0 | 1 | 0 | <0.001 | 44 (44-44) | 0.53 |
| MIA | 0 | 0 | 3 | | 0 | 1 | 2 | 0 | | 0 | 0 | 1 | 1 | | 16 (8-22) | |
| IA with predominant lepidic component | 0 | 7 | 12 | | 0 | 12 | 5 | 2 | | 0 | 6 | 2 | 9 | | 20 (5-160) | |
| IA without predominant lepidic pattern | 1 | 1 | 21 | | 1 | 18 | 4 | 0 | | 0 | 2 | 1 | 18 | | 25 (4-250) | |
| Collapse | | | | | | | | | | | | | | | | |
| Absent | 0 | 1 | 13 | 0.29 | 0 | 11 | 3 | 0 | 0.51 | 0 | 2 | 1 | 10 | 0.76 | 19 (4-250) | 0.53 |
| Present | 2 | 7 | 24 | | 2 | 20 | 9 | 2 | | 1 | 6 | 4 | 18 | | 21 (5-160) | |
| Maximum size of invasive component (mm) | | | | | | | | | | | | | | | | |
| ≤10 | 1 | 5 | 11 | 0.45 | 1 | 9 | 6 | 1 | 0.80 | 1 | 4 | 3 | 5 | 0.039 | 14 (4-160) | 0.003 |
| 11-20 | 0 | 1 | 6 | | 0 | 5 | 2 | 0 | | 0 | 2 | 2 | 2 | | 13 (7-137) | |
| 21-30 | 0 | 2 | 8 | | 0 | 8 | 1 | 1 | | 0 | 2 | 0 | 8 | | 24 (11-105) | |
| >30 | 1 | 0 | 12 | | 1 | 9 | 3 | 0 | | 0 | 0 | 0 | 13 | | 45 (19-250) | |

IA has been split into two categories: with and without predominant lepidic pattern.
[a]FDG uptake was addressed as a semiquantitative evaluation.
HR-CT, high-resolution computed tomography; PET-CT, positron emission tomography-computed tomography; GGO, ground-glass opacity; GGN, ground-glass nodule; SN, solid nodule; SM, smooth; SP, spiculated; LB, lobulated; No M, no margins; NU, no uptake; F, faint; MOD, moderate; INT, intense; AIS, adenocarcinoma in situ; MIA, minimally invasive adenocarcinoma; FDG, fluorodeoxyglucose; IA, Invasive adenocarcinoma.

completely solid lesions, which histologically corresponds to the collapse of the predominant lepidic tumor growth pattern.

In the current literature, the solid component on HR-CT in pulmonary adenocarcinoma is associated with invasive cancer, a finding supported by microscopic evidence of invasion and lymph-node involvement.[8] In nonneoplastic pulmonary lesions, a solid appearance on HR-CT images was explained by microscopic collapse of lung parenchyma.[23] The current WHO classification of lung cancer[7] does not take collapse of peripheral lung tissue with tumor cells into account for adenocarcinoma criteria. The term *collapse* in relation to pulmonary nonmucinous adenocarcinoma was described in 1980 by Shimosato et al.[24] as a description of a pattern of growth. Subsequently, in 1995, Noguchi et al.[25] described an AIS of the lung in relation to collapse and interstitial thickening, with a replacement growth pattern and slightly fibrotic foci. Recently, the term *collapse*, as described in Figure 1, was used to denote loss of air in the alveolar spaces compared with physiologically expanded alveoli owing to an alteration of the flexibility of the peripheral lung tissue[26] not only during ventilation but also owing to handling of biopsies and resection specimens.

Lesions with a solid appearance on HR-CT images can also be benign, such as in organizing pneumonia, nonspecific fibrosis, and aspergillosis.[27-29] Our study reveals that the solid appearance may be owing to the reduction of air in the alveolar spaces and occasionally in combination with partial alveolar filling by inflammatory cells, such as neutrophils and macrophages. The latter have been found previously.[27] A three-dimensional reconstruction study revealed that a tumor with a microscopic, seemingly papillary appearance may be erroneously classified as papillary carcinoma, although the proper diagnosis is predominant lepidic adenocarcinoma with collapse.[30] Thus, our radiologic-pathologic comparison study reveals that the in vivo collapse of predominant lepidic adenocarcinoma and AIS can result in a partially or completely solid lesion on radiologic examination, a phenomenon called tumor atelectasis.

In HR-CT imaging, collapse of the peripheral lung tissue has for a long time been recognized as atelectasis owing to repression or reduction of air, which corresponds with Hounsfield units of +100 to −100.[31,32] Occasional cases in other studies with radiologic and pathologic correlation reported hints of tumor atelectasis.[16,33] In our study, without restriction on tumor size, a collapse in lepidic growth pattern of adenocarcinoma was observed in 69% of the resected adenocarcinomas, explaining at least a part of the radiologic solid component observed as tumor atelectasis. Previous studies evaluated a variety of radiologic parameters, such as

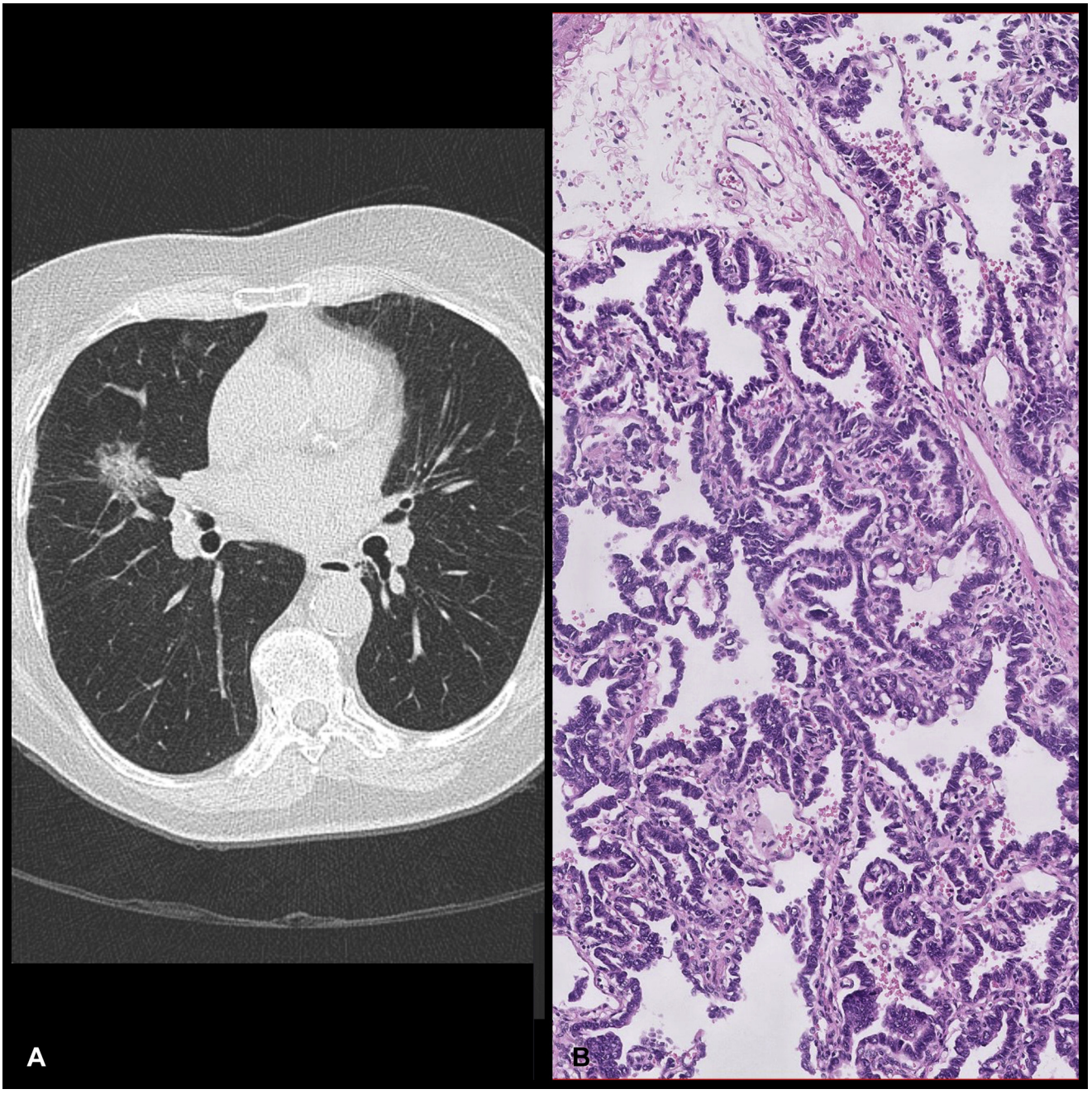


**Figure 2.** High-resolution computed tomography (*A*) revealed a single ground-glass component nodule, and the histologic examination (*B*) revealed an adenocarcinoma in situ (×200 magnification, hematoxylin and eosin).

attenuation, association with a GGO, the size of the solid component if it was similar to the size of the GGN, and the presence of air bronchogram; all these were associated with invasive adenocarcinoma.[16,34] However, none of these studies take into account tumor atelectasis as a possible cause of solid appearance on CT scan.

In pathophysiologic terms, tumor atelectasis can be explained by increased stiffness of the pulmonary tissue owing to the coverage by tumor cells on the initially thin flexible alveolar walls. During inspiration, the higher resistance leads to less air flow in the tumor areas compared with the adjacent lung parenchyma.[35] Radiologically, this effect is most likely in the center of the tumor and more prominently if inflammatory cells (macrophages associated with edema) and slight fibrosis are also present. Noteworthy, from a pathologic viewpoint, the collapse in the histologic sections can occur in vivo and ex vivo.[32] Importantly, any morphologic sign of invasion was lacking in the collapsed areas in which the corresponding radiologic appearance was solid. This

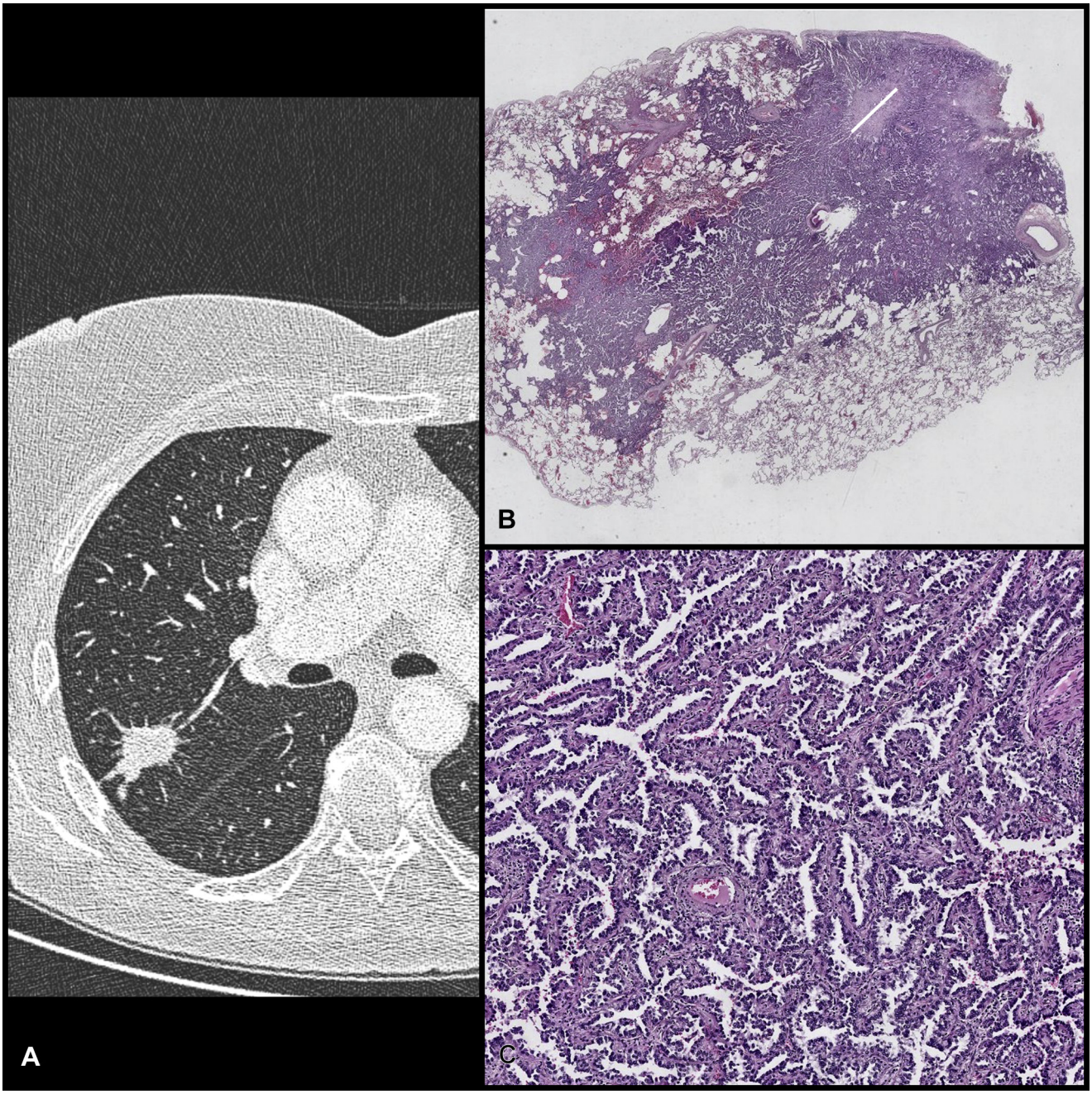


**Figure 3.** High-resolution computed tomography (*A*) revealed a single SN, and the histologic examination (hematoxylin and eosin stain, [*B*] ×50 and inset [*C*] ×200 magnification) revealed a minimally invasive adenocarcinoma. Note the prominent large solid component (tumor atelectasis) in high-resolution computed tomography and a predominant lepidic component with collapse in histology. The white bar denotes the invasive component (≤5 mm).

demonstrates the presence of AIS tumor atelectasis in vivo.

In our study, tumor atelectasis matched histologically with AIS, MIA, or adenocarcinoma, with a predominant lepidic pattern of growth. The radiologic images of tumor atelectasis were GGO, GGN, and SN.

Furthermore, in line with previous results, our study confirms a significant ($p = 0.003$) association among radiologic classifications of lung nodules, GGO, GGN, and SN, on HR-CT imaging with AIS, MIA, and IA, respectively.[13] Likewise, spiculated margins were associated with IA, in contrast to lobulated and smooth margins associated with AIS and MIA.[36] The study of Wang et al.[33] analyzed pulmonary lesions with a solid component, classified as mixed GGN. The frequency found is dependent on selection: 7.5% resulted in

preinvasive adenocarcinoma of the lung, which includes atypical adenomatous hyperplasia and AIS.

Tanaka et al.[37] identified 4.3 as the optimal cutoff value of $SUV_{max}$ to determine pleural invasion, and in the present investigation, $SUV_{max}$ correlated with histologic pleural invasion status. Other PET-CT results confirm previous investigations.[38] This study reveals a significant association between both the visual analysis of FDG uptake (Table 3) and the visual FDG uptake and the selected pleural invasion on histologic section ($p = 0.001$). The $SUV_{max}$ values found in the present study cannot be directly compared with those in the study of Tanaka et al.,[37] as in our study, the acquisition of the images was started 60 minutes postinjection (in the study of Tanaka et al.,[37] this was 90 min). SUV values increase over time after injection. Especially in small lesions, a partial volume effect may result in an underestimation of the SUV value. In clinical practice, FDG uptake in pulmonary lesions is usually evaluated by visual evaluation. Furthermore, PET-CT evaluation did not support the discrimination between an invasive component of adenocarcinoma and tumor atelectasis; indeed, both resulted in PET positivity.

The presence of a solid component in SN and GGN on HR-CT imaging is usually considered to be a parameter with poor prognosis in pulmonary adenocarcinoma.[13,39,40] According to Tsutani et al.,[39] the prognostic significance of the solid component in HR-CT imaging, closely related to $SUV_{max}$, has been reported to be a feature of invasion in HR-CT. In contrast, according to Hattori et al.,[34] the presence of a GGO component had a strong influence on the prognosis, more than the size of the solid component. Ye et al.[15] also found a better survival in patients with subsolid appearance compared with those with solid tumors on HR-CT imaging but had no prognostic features in the subsolid nodules. Possibly, tumor atelectasis may provide an explanation for this finding.

Our investigation has limitations as a retrospective study: not all patient image data could be retrieved. In addition, this recent cohort has no follow-up data.

In summary, only on the basis of HR-CT features of nodules, the solid component should not be interpreted with certainty as invasive cancer, and tumor atelectasis should also be taken into account as an underlying possibility.

## Supplementary Data

Note: To access the supplementary material accompanying this article, visit the online version of the *Journal of Thoracic Oncology Clinical and Research Reports* at www.jtocrr.org and at https://doi.org/10.1016/j.jtocrr.2020.100018.

## References


1. Reck M, Rabe KF. Precision diagnosis and treatment for advanced non-small-cell lung cancer. *N Engl J Med*. 2017;377:849–861.
2. Naidich DP, Bankier AA, MacMahon H, et al. Recommendations for the management of subsolid pulmonary nodules detected at CT: a statement from the Fleischner Society. *Radiology*. 2013;266:304–317.
3. Hansell DM, Bankier AA, MacMahon H, McLoud TC, Müller NL, Remy J. Fleischner Society: glossary of terms for thoracic imaging. *Radiology*. 2008;246:697–722.
4. Chung K, Ciompi F, Scholten ET, et al. Visual discrimination of screen-detected persistent from transient subsolid nodules: an observer study. *PLoS One*. 2018;13:e0191874.
5. Webb WR. Thin-section CT of the secondary pulmonary lobule: anatomy and the image—the 2004 Fleischner lecture. *Radiology*. 2006;239:322–338.
6. Leslie KO, Yousem SA, Colby TV. Lungs. In: Mills SE (ed.) Histology for pathologists. 4th ed. Philadelphia, PA: *Wolters Kluwer*; 2012:505–541.
7. Travis WD, Brambilla E, Nicholson AG, et al. The 2015 World Health Organization classification of lung tumors. *J Thorac Oncol*. 2015;10:1243–1260.
8. Hayashi H, Ashizawa K, Ogihara Y, et al. Comparison between solid component size on thin-section CT and pathologic lymph node metastasis and local invasion in T1 lung adenocarcinoma. *Jpn J Radiol*. 2017;35:109–115.
9. Saji H, Matsubayashi J, Akata S, et al. Correlation between whole tumor size and solid component size on high-resolution computed tomography in the prediction of the degree of pathologic malignancy and the prognostic outcome in primary lung adenocarcinoma. *Acta Radiol*. 2015;56:1187–1195.
10. Travis WD, Asamura H, Bankier AA, et al. The IASLC lung cancer staging project: proposals for coding T categories for subsolid nodules and assessment of tumor size in part-solid tumors in the forthcoming eighth edition of the TNM classification of lung cancer. J Thorac *Oncol*. 2016;11:1204–1223.
11. Suzuki K, Koike T, Asakawa T, et al. A prospective radiological study of thin-section computed tomography to predict pathological noninvasiveness in peripheral clinical IA lung cancer (Japan Clinical Oncology Group 0201). *J Thorac Oncol*. 2011;6:751–756.
12. Shimizu K, Yamada K, Saito H, et al. Surgically curable peripheral lung carcinoma: correlation of thin-section CT findings with histologic prognostic factors and survival. *Chest*. 2005;127:871–878.
13. Kudo Y, Matsubayashi J, Saji H, et al. Association between high-resolution computed tomography findings and the IASLC/ATS/ERS classification of small lung adenocarcinomas in Japanese patients. *Lung Cancer*. 2015;90:47–54.
14. Matsuguma H, Oki I, Nakahara R, et al. Comparison of three measurements on computed tomography for the prediction of less invasiveness in patients with clinical stage I non-small cell lung cancer. *Ann Thorac Surg*. 2013;95:1878–1884.
15. Ye T, Deng L, Wang S, et al. Lung adenocarcinomas manifesting as radiological part-solid nodules define a special clinical subtype. *J Thorac Oncol*. 2019;14:617–627.
16. Lim H, Ahn S, Lee KS, et al. Persistent pure ground-glass opacity lung nodules $\geq$ 10 mm in diameter at CT scan: histopathologic comparisons and prognostic implications. *Chest*. 2013;144:1291–1299.

17. Kadota K, Villena-Vargas J, Yoshizawa A, et al. Prognostic significance of adenocarcinoma in situ, minimally invasive adenocarcinoma, and nonmucinous lepidic predominant invasive adenocarcinoma of the lung in patients with stage I disease. *Am J Surg Pathol*. 2014;38:448–460.
18. Kadota K, Yeh Y-C, Sima CS, et al. The cribriform pattern identifies a subset of acinar predominant tumors with poor prognosis in patients with stage I lung adenocarcinoma: a conceptual proposal to classify cribriform predominant tumors as a distinct histologic subtype. *Mod Pathol*. 2014;27:690–700.
19. Thunnissen E, Beasley MB, Borczuk AC, et al. Reproducibility of histopathological subtypes and invasion in pulmonary adenocarcinoma. An international interobserver study. *Mod Pathol*. 2012;25:1574–1583.
20. Radonic T, Dickhoff C, Mino-Kenudson M, Lely R, Paul R, Thunnissen E. Gross handling of pulmonary resection specimen: maintaining the 3-dimensional orientation. *J Thorac Dis*. 2019;11(suppl 1):S37–S44.
21. Amin MB, Edge S, Greene F, et al. *AJCC Cancer Staging Manual*. 8th ed. Chicago, IL: Springer International Publishing, American College of Surgeons; 2017.
22. ter Wee MM, Lissenberg-Witte BI. *A Quick Guide on How to Conduct Medical Research: From Set-Up to Publication*. Houten: Bohn Stafleu van Loghem; 2019.
23. McHugh K, Blaquiere RM. CT features of rounded atelectasis. *Am J Roentgenol*. 1989;153:257–260.
24. Shimosato Y, Suzuki A, Hashimoto T, et al. Prognostic implications of fibrotic focus (scar) in small peripheral lung cancers. *Am J Surg Pathol*. 1980;4:365–373.
25. Noguchi M, Morikawa A, Kawasaki M, et al. Small adenocarcinoma of the lung. Histologic characteristics and prognosis. *Cancer*. 1995;75:2844–2852.
26. Thunnissen E, Blaauwgeers HJ, de Cuba EM, Yick CY, Flieder DB. Ex vivo artifacts and histopathologic pitfalls in the lung. *Arch Pathol Lab Med*. 2016;140:212–220.
27. Watanabe K, Harada T, Yoshida M, et al. Organizing pneumonia presenting as a solitary nodular shadow on a chest radiograph. *Respiration*. 2003;70:507–514.
28. Park CM, Goo JM, Lee HJ, Lee CH, Chun EJ, Im JG. Nodular ground-glass opacity at thin-section CT: histologic correlation and evaluation of change at follow-up. *Radiographics*. 2007;27:391–408.
29. Furuya K, Yasumori K, Takeo S, et al. Lung CT: part 1, mimickers of lung cancer—spectrum of CT findings with pathologic correlation. *AJR Am J Roentgenol*. 2012;199:W454–W463.
30. Thunnissen E, Beliën JA, Kerr K, et al. In compressed lung tissue microscopic sections of adenocarcinoma in situ may mimic papillary adenocarcinoma. *Arch Pathol Lab Med*. 2013;137:1792–1797.
31. Lohser J, Slinger P. Lung injury after one-lung ventilation: a review of the pathophysiologic mechanisms affecting the ventilated and the collapsed lung. *Anesth Analg*. 2015;121:302–318.
32. Rylander C, Hogman M, Perchiazzi G, Magnusson A, Hedenstierna G. Functional residual capacity and respiratory mechanics as indicators of aeration and collapse in experimental lung injury. *Anesth Analg*. 2004;98:782–789.
33. Wang X, Chen W, He W, et al. CT features differentiating pre- and minimally invasive from invasive adenocarcinoma appearing as mixed ground-glass nodules: mass is a potential imaging biomarker. *Clin Radiol*. 2018;73:546–554.
34. Hattori A, Matsunaga T, Takamochi K, Oh S, Suzuki K. Importance of ground glass opacity component in clinical stage IA radiologic invasive lung cancer. *Ann Thorac Surg*. 2017;104:313–320.
35. Henschke CI, Yankelevitz DF, Mirtcheva R, et al. CT Screening for lung cancer: frequency and significance of part-solid and nonsolid nodules. *AJR Am J Roentgenol*. 2002;178:1053–1057.
36. Han D, Heuvelmans MA, Vliegenthart R, et al. Influence of lung nodule margin on volume- and diameter-based reader variability in CT lung cancer screening. *Br J Radiol*. 2018;91:20170405.
37. Tanaka T, Shinya T, Sato S, et al. Predicting pleural invasion using HRCT and 18F-FDG PET/CT in lung adenocarcinoma with pleural contact. *Ann Nucl Med*. 2015;29:757–765.
38. Nishii K, Bessho A, Fukamatsu N, et al. Statistical analysis of 18F-fluorodeoxyglucose positron-emission tomography/computed tomography ground-glass nodule findings. *Mol Clin Oncol*. 2018;9:279–282.
39. Tsutani Y, Miyata Y, Nakayama H, et al. Prognostic significance of using solid versus whole tumor size on high-resolution computed tomography for predicting pathologic malignant grade of tumors in clinical stage IA lung adenocarcinoma: a multicenter study. *J Thorac Cardiovasc Surg*. 2012;143:607–612.
40. Zhang Y, Shen Y, Qiang JW, Ye JD, Zhang J, Zhao RY. HRCT features distinguishing pre-invasive from invasive pulmonary adenocarcinomas appearing as ground-glass nodules. *Eur Radiol*. 2016;26:2921–2928.